THE EFFICIENCY OF I-BEAM STEEL SECTION WITH PERFORATED-CORRUGATED WEB PROFILE

HAZWANI BINTI HASAN

UNIVERSITI SAINS MALAYSIA

2017

THE EFFICIENCY OF I-BEAM STEEL SECTION WITH PERFORATED-CORRUGATED WEB PROFILE

by

HAZWANI BINTI HASAN

Thesis submitted in fulfillment of the requirements for the degree of Master of Science

March 2017

ACKNOWLEDGEMENTS

First and foremost, I would like to express my deepest appreciation to my supervisor, Assoc. Prof. Dr. Fatimah De'nan for her continuous guidance, thoughtful supervision and valuable suggestions which enable me to complete this research work successfully.

Furthermore, I would also like to acknowledge with much appreciation to Assoc. Prof. Dr. Choong Kok Keong who has contributed in stimulating the suggestion and encouragement, and also helps in writing this thesis. The comments and cooperation's were crucial for the success of this research.

I would also like to thank Universiti Sains Malaysia for providing me the best facilities and conducive environment throughout my postgraduate study and thanks to Research University Grant (RUI) (Account Number: 1001/PAWAM/814222) in funding this project.

Special thanks to all my friends, Ms Aiin Aziz especially, Ms Nisha Omar, Ms Farhah Naim, and Ms Aqilah and other colleagues for their continuous support, commitment and help during the period of the research.

My sincere gratitude and deepest appreciation to my husband, Muhamad Fadzli for his patience, support and advice which enable me to complete this research work successfully and to my family members, whose continuously support and encourage for my long-life journey of learning. I am also indebted to every individual for their involvement directly and indirectly throughout this research. I really appreciate their relevant comments and encouragement during my research period. Thank you for always being there and making this pursuit a valuable journey.

TABLE OF CONTENTS

	Page
ACKNOWLEDGEMENTS	ii
TABLE OF CONTENTS	iii
LIST OF TABLES	vii
LIST OF FIGURES	ix
LIST OF SYMBOLS	xiii
LIST OF ABBREVIATIONS	xv
ABSTRAK	xvi
ABSTRACT	xviii
CHAPTER ONE: INTRODUCTION	
1.1 Introduction	1
1.2 Structural efficiency	1
1.3 Types of steel section	2
1.3.1 Corrugated steel section	2
1.3.2 Perforated steel section	5
1.4 Problem statement	6
1.5 Objectives	10
1.6 Scope of work	10
1.7 Thesis organisation	11

CHAPTER TWO: LITERATURE REVIEW

2.1 Perforated steel section 12

2.1.1 Structural behaviour and performance of perforated steel section 17

2.1.1.1 Buckling study 18

2.1.1.2 Shear behaviour and strength 21

2.1.1.3 Bending resistance and ultimate strength 27

2.1.1.4 Torsional resistance 30

2.2 Corrugated steel section 31

2.2.1 Structural behaviour and performance of corrugated member 32

2.2.1.1 Shear behaviour and strength 32

2.2.1.2 Bending and buckling behaviour 34

2.2.1.3 Torsional behaviour 39

2.3 Summary 42

CHAPTER THREE: METHODOLOGY

3.1 Framework of research study 48

3.2 Model description 51

3.2.1 Section properties 51

3.2.2 Perforation shapes and sizes 52

3.2.3 Layouts of perforation 55

3.3 Determination of structural efficiency 56

3.4 Numerical study 58

3.4.1 Material properties 58

3.4.2 Shell element 60

3.4.3 Buckling analysis 61

3.5 Convergence study 62

3.6 Support and loading position 63

3.6.1 Shear loading condition 64

3.6.2 Torsional loading condition 65

3.6.3 Bending loading condition 66

3.6.4 Lateral torsional buckling loading condition 67

3.7 Parametric study 67

3.7.1 Effect of web thickness, t_w 68

3.7.2 Effect of flange thickness, t_f 69

CHAPTER FOUR: RESULTS AND DISCUSSION

4.0 Overview 71

4.1 Model selfweight and weight reduction 70

4.2 Stage 1: Determination of the most efficient perforation shape, size and layout under different loading condition 74

4.2.1 Bending loading condition 75

4.2.2 Lateral torsional buckling loading condition 82

4.2.3 Torsional loading condition 88

4.2.4 Shear loading condition 95

4.3 Stage 2: Effect of different section parameter and span length on structural performance of model under different loading condition 101

4.3.1 Bending loading condition 102

4.3.2 Lateral torsional buckling loading condition 103

4.3.3 Torsional loading condition 105

4.3.4 Shear loading condition 108

4.4 Summary 110

CHAPTER FIVE: CONCLUSIONS AND RECOMMENDATIONS

5.1 Conclusions 111

5.2 Recommendations for future work 112

REFERENCES 113

APPENDICES

APPENDIX A (Results of bending loading condition in Stage 1)

APPENDIX B (Results of lateral torsional buckling loading condition in Stage 1)

APPENDIX C (Results of torsional loading condition in Stage 1)

APPENDIX D (Results of shear loading condition in Stage 1)

APPENDIX E (Theory of torsional rotation)

LIST OF PUBLICATIONS

LIST OF TABLES

		Page
Table 2.1	Literature review for corrugated steel section	43
Table 2.2	Literature review for perforated steel section	45
Table 3.1	The dimensional properties of TriWP with and without perforation	51
Table 3.2	Result of tensile test	59
Table 3.3	Summary of material properties from tensile test	59
Table 3.4	Maximum nodal displacements with different mesh sizes	63
Table 3.5	Model with different web thickness	68
Table 3.6	Model at different flange thickness	69
Table 4.1	Selfweight of TriWP with perforation for Layout 1	71
Table 4.2	Self -weight of TriWP with perforation for Layout 2	71
Table 4.3	Self -weight of TriWP with perforation for Layout 3	72
Table 4.4	Percentage difference of weight reduction of TriWP with perforation for Layout 1	73
Table 4.5	Percentage difference of weight reduction of TriWP with perforation for Layout 2	73
Table 4.6	Percentage difference of weight reduction of TriWP with perforation for Layout 3	73
Table 4.7	Results of load at yield, P_y for all TriWP with perforation	81
Table 4.8	Structural efficiency of TriWP with perforation	81
Table 4.9	Percentage difference of structural efficiency	81
Table 4.10	The Buckling load of TriWP with perforation	83
Table 4.11	Moment buckling resistance of TriWP with perforation	84
Table 4.12	Percentage difference of moment buckling resistance	84

Table 4.13	Structural efficiency of TriWP with perforation	87
Table 4.14	The percentage difference of structural efficiency	87
Table 4.15	Torsional rotation for TriWP with perforation of circular shaped	89
Table 4.16	Torsional rotation for TriWP with perforation of square shaped	89
Table 4.17	Torsional rotation for TriWP with perforation of hexagonal shaped	89
Table 4.18	Torsional rotation for TriWP with perforation of diamond shaped	90
Table 4.19	Torsional rotation for TriWP with perforation of diamond shaped	90
Table 4.20	Results of load at yield, P_y of TriWP with perforation	94
Table 4.21	Structural efficiency of TriWP with perforation	94
Table 4.22	Percentage difference of structural efficiency	95
Table 4.23	The percentage difference of shear buckling capacity	96
Table 4.24	The structural efficiency of TriWP with perforation	99
Table 4.25	Percentage difference of structural efficiency	99
Table 4.26	Shear buckling capacity of TriWP with perforation of diamond in shape and 0.4D in size arranged in Layout 3	108

LIST OF FIGURES

		Page
Figure 1.1	I-beam with stiffener plate (Sayed-Ahmed, 2007)	3
Figure 1.2	Profile of hexagonal sectional shape corrugated web (Oh et al., (2012)	3
Figure 1.3	Trapezoidal profile of the corrugated web plates (Sayed-Ahmed, 2007)	4
Figure 1.4	Profile of curved corrugated web (Eldib, 2009)	4
Figure 1.5	Profile of Triangular Web Profile (De'nan & Hashim, 2012)	5
Figure 1.6	Common type of web opening (Siddh and Pachpor, 2011)	6
Figure 1.7	Conventional I-beam	7
Figure 1.8	Profiles of I-girder with corrugated webs and global coordinates of corrugation profile (Moon et al. (2009))	8
Figure 2.1	Important areas and geometrical key parameters (Tsavdaris et al., 2012)	13
Figure 2.2	Vierendeel mechanism and location of plastic hinge (Chung et al., 2000)	15
Figure 2.3	Development of the fillet corner web opening shape (Wang et al., 2014)	16
Figure 2.4	Stress distributions of unit members with the different shapes of the web openings (Wang et al., 2014)	16
Figure 2.5	Steel I-beam with opening (a) beam and opening parameters, and (b) finite element model in un-deformed shape, sample lateral buckling (LB) mode and LTB mode (Serror, 2011)	18
Figure 2.6	Critical buckling mode by FEA-ADAPTIC and EFG/RSA models (Abidin and Izzudin, 2013)	20
Figure 2.7	'Strut' model of web-post model (Tsavdaris and Mello, 2011)	22
Figure 2.8	Typical web-post behaviour (Tsavdaris and Mello, 2011)	22
Figure 2.9	Comparison of normalized yield strengths of models plotted against perforation ratio A_h/A_g (Chan et al. 2013)	23

Figure 2.10	A typical girder on the test rig (Darehsouri et al., 2013)	23
Figure 2.11	Experimental set-up of back LCBs with web openings (Mahendran and Keerthan, 2013)	25
Figure 2.12	FE mesh for a typical HTFPG with web opening (Hassanein, 2014)	26
Figure 2.13	Shear load-mid span deflection curves for all tested panels (Hamoodi and Gabar, 2013)	27
Figure 2.14	Deflection and von mises stress for the specific position of web opening (Siddh and Pachpor, 2011)	28
Figure 2.15	Ultimate Failure of 200 x 45 x 1.6 LSB (span = 4m, hole diameter = 127 mm, spacing S = 500 mm) (Seo and Mahendran, 2012)	29
Figure 2.16	Three different shear buckling modes of trapezoidal corrugated steel webs (Nie et al., 2013)	34
Figure 2.17	Geometry of model (Khalid et al., 2004)	35
Figure 2.18	The test specimen (Osman et al., 2007)	35
Figure 2.19	The overall view of the test beam (Denan et al., 2010)	39
Figure 2.20	The buckling shape mode (Denan et al., 2010)	39
Figure 2.21	Torsion versus torsional rotation θ_2 for FW 3c, FW 3d, TriWP 3c and TriWP 3d (Denan et al., 2015)	41
Figure 3.1	Flow chart of the research study	50
Figure 3.2	Profile of TriWP with perforation	52
Figure 3.3	TriWP with perforation of circular shaped	53
Figure 3.4	TriWP with perforation of square shaped	53
Figure 3.5	TriWP with perforation of hexagonal shaped	53
Figure 3.6	TriWP with perforation of diamond shaped	54
Figure 3.7	TriWP with perforation of octagonal shaped	54

Figure 3.8	The isometric view of TriWP with perforation of circular shaped arranged in Layout 1	55
Figure 3.9	The isometric view of TriWP with perforation of circular shaped arranged in Layout 2	56
Figure 3.10	The isometric view of TriWP with perforation of circular shaped arranged in Layout 3	56
Figure 3.11	Stress strain curve of steel plate 1	59
Figure 3.12	Triangular thin shell element (TSL6) and Quadrilateral thin shell element (QSL8)	60
Figure 3.13	Graph of displacement against number of elements	63
Figure 3.14	Supports and loading position of model for shear loading condition	64
Figure 3.15	Supports and loading positions of model for torsional loading condition	65
Figure 3.16	Supports and loading position of model for bending and lateral torsional buckling loading conditions	66
Figure 4.1	The deflection of TriWP with perforation size of (a) 0.4D, (b) 0.5D and (c) 0.6D at 10 kN	76
Figure 4.2	The displacement contour for TriWP with perforation of diamond in shape and 0.4D in size under bending loading condition (10 kN)	77
Figure 4.3	Load versus deflection for TriWP with perforation of diamond shaped for (a) Layout 1, (b) Layout 2 and (c) Layout 3	79
Figure 4.4	Load at yield, P_y of TriWP without perforation	80
Figure 4.5	The contour of displacement for TriWP with perforation of diamond in shape and 0.4D in size under lateral torsional buckling loading condition (10 kN)	85
Figure 4.6	The contour of displacement for TriWP with diamond perforation of 0.4D under torsional loading condition (10 kN)	91
Figure 4.7	Load versus torsional rotation of TriWP with perforation of diamond in shape and 0.4D in size arranged in (a) Layout 1, (b) Layout 2 and (c) Layout 3	93

Figure 4.8	Shear buckling capacity of TriWP with perforation of (a) 0.4D, 0.5D and 0.6D	97
Figure 4.9	Result of contour for TriWP with perforation of diamond in shape and 0.4D in size for Mode 1	100
Figure 4.10	Deflection versus flange thickness for TriWP with perforation of diamond in shape and 0.4D in size arrange in Layout 3	102
Figure 4.11	Deflection versus web thickness for TriWP with perforation of diamond in shape and 0.4D in size arrange in Layout 3	103
Figure 4.12	$M_{b,Rd}$ flange thickness for TriWP with perforation of diamond in shape and 0.4D in size arrange in Layout 3	104
Figure 4.13	$M_{b,Rd}$ versus web thickness for TriWP with perforation of diamond in shape and 0.4D in size arrange in Layout 3	105
Figure 4.14	Torsional rotation versus flange thickness for TriWP with perforation of diamond in shape and 0.4D in size arrange in Layout 3	106
Figure 4.15	Torsional rotation versus web thickness for TriWP with perforation of diamond in shape and 0.4D in size arrange in Layout 3	107
Figure 4.16	Shear buckling capacity versus D/t_w of model	109

LIST OF SYMBOLS

D	Depth of the web section
B	Flange width
t_w	Web thickness
t_f	Flange thickness
L	Span length
δ	Deflection
P_y	Load at yield
P_b	Buckling load
θ	Torsional rotation
$M_{b,Rd}$	Buckling resistance moment
W	Point load
γ_{M1}	Partial safety factor
E	Modulus of elasticity
I	Moment of inertia
χ_{LT}	Buckling factor
α_{LT}	Imperfection factor
W_y	Bending resistance corresponding to the cross-section classification of the member
f_y	Yield strength of steel
M_{cr}	Elastic critical moment
T_q	The applied torque

z	The length of member subjected to T_q
G	Modulus of rigidity
J	Torsional constant
A_v	Shear area
f_{yw}	Yield strength of the web
L_{cr}	Length of beam between points which have lateral restraint
I_z	Second moment of area about the minor axis
I_y	Second moment of area about the major axis
I_t	Torsional constant
I_w	Warping constant

LIST OF ABBREVIATIONS

TriWP	Triangular web profile
FW	Flat web
LTB	Lateral torsional buckling
LB	Local buckling
TWP	Trapezoidal web profile
FE	Finite element

KECEKAPAN KERATAN RASUK-I KELULI DENGAN PROFIL WEB BUKAAN-BERALUN

ABSTRAK

Kajian ini mengkaji kecekapan struktur keratan rasuk- I keluli berprofil web segi tiga (TriWP) berlubang. Dua peringkat analisis telah dibuat dengan menganalisis 359 model. Di Peringkat 1, kecekapan struktur rasuk TriWP dengan bukaan yang berdimensi 200 mm × 100 mm × 6 mm × 4 mm dan panjang rentang kira-kira 900 mm ditentukan berdasarkan nisbah kapasiti beban kepada berat sendiri. Ia dikira di bawah keadaan saiz lubang yang berbeza iaitu 0.4D, 0.5D dan 0.6D; lima bentuk bukaan yang berbeza iaitu bulat, segiempat sama, heksagon, oktagon dan berlian dan susun atur bukaan yang berbeza (Susun atur 1, Susun atur 2 dan Susun atur 3). Dengan menggunakan kombinasi ini, analisis model dilaksanakan untuk keadaan lenturan, lengkokan kilasan sisi, kilasan dan ricih pada peringkat kedua kajian. Pada peringkat ini, bentuk, saiz dan susun atur bukaan yang paling cekap dipilih berdasarkan kepada nilai kecekapan struktur tertinggi. TriWP dengan bukaan bersaiz 0.4D, bukaan berbentuk berlian dan susun atur bukaan pada Susun atur 3 menunjukkan kecekapan struktur yang tertinggi berbanding model-model lain. Nilai-nilai tersebut masing-masing ialah 158.63, 799.0, 132.17 dan 204.75 dibawah keadaan beban seperti kelakuan lentur, lengkokan kilasan sisi, kilasan dan ricih. Di Peringkat 2, ketebalan web yang berbeza, ketebalan bebibir dan panjang rentang yang digunakan pada model yang dipilih dalam Peringkat 1 untuk memerhati prestasi dan tingkah laku di bawah empat keadaan beban iaitu lenturan, lengkokan kilasan sisi, kilasan dan ricih. Didapati bahawa apabila web dan ketebalan bebibir meningkat di bawah panjang rentang yang sama dengan lebar bebibir dan kedalaman web yang sama, nilai pesongan dan putaran

kilasan model masing-masing menurun di bawah keadaan beban lenturan dan kilasan. Walau bagaimanapun, nilai-nilai (pesongan dan putaran kilasan) didapati meningkat apabila panjang rentang yang meningkat. Selain itu, nilai kapasiti lengkokan ricih meningkat di bawah keadaan beban ricih dan nilai momen rintangan lengkokan juga didapati meningkat di bawah keadaan beban lengkokan sisi kilasan. Walau bagaimanapun, nilai keupayaan lengkokan ricih dan rintangan lengkokan didapati berkurangan apabila panjang rentang meningkat.

THE EFFICIENCY OF I-BEAM STEEL SECTION WITH PERFORATED-CORRUGATED WEB PROFILE

ABSTRACT

This study investigates the structural efficiency of the triangular web profile (TriWP) steel section with perforation. Two stages were included which comprised of 359 models that were analysed. In Stage 1, the structural efficiency of the TriWP with perforation with the dimension of 200 mm × 100 mm × 6 mm × 4 mm and span length of 900 mm is determined from the ratio of load carrying capacity to selfweight. It is calculated under the condition of different perforation sizes i.e. 0.4D, 0.5D and 0.6D; five different perforation shapes which are circular, square, hexagonal, diamond and octagonal and three different layouts of perforations (Layout 1, Layout 2 and Layout 3). By using these combinations, the analysis of the model subjected to loading causing bending, lateral torsional buckling, torsion and shear are analysed. In this stage, the most efficient perforation shape, size and layout is selected based on the highest value of structural efficiency. TriWP with the perforation size of 0.4D, diamond perforation shape arranged in Layout 3 is found to shows the highest structural efficiency value compared to other models. The values are 158.63, 799.0, 132.17 and 204.75 for bending, lateral torsional buckling, torsion and shear loading conditions, respectively. In Stage 2, different web thickness, flange thickness and span length are used on the selected model in Stage 1 to observe the performance and its behaviour under four loading condition i.e. bending, lateral torsional buckling, torsion and shear. It is found that when the web and flange thickness are increased under the same span length with constant flange width and web depth, the value of deflection and torsional rotation of model decreased under bending and torsional loading conditions, respectively.

Nevertheless, these values (deflection and torsional rotation) are found to increase when the span length increased. Moreover, the value of shear buckling capacity of model is increased under shear loading condition and the value of moment buckling resistance is also found to increase under loading causing lateral torsional buckling. Nevertheless, the value of shear buckling capacity and moment buckling resistance are found to decrease when the span length increased.

CHAPTER ONE

INTRODUCTION

1.1 Introduction

Development of new material and innovation in construction technology always give birth to the novel structure which satisfies the increasingly diversified demand such as economy, durability and world-wide environmental requirements. Bridges, airports, stadium, skyscrapers and other modern infrastructures are supported by a steel skeleton. There are many advantages of using steel in construction such as the excellent strength to weight ratio, easily connected metal joist, and the availability of various shapes of the structural steel element. Despite these advantages, there are also some challenges which are best solved by a better understanding of how the metals actually perform in a structure. For larger buildings, metals are the key element of the structural system. Steel beams and columns, steel joists, steel studs, aluminium framing are the few examples of metal construction elements (Ram, 2010).

1.2 Structural efficiency

Structural efficiency is measured in terms of weight of material which has to be provided to carry a given amount of load. The efficiency of a structure is regarded as high if the ratio of load carrying capacity to its weight is high. The weight of material required for a structure dependent principally on its overall form in relation to the pattern of applied load and on the shapes of structural elements.

It is possible to specify precisely the level of structural efficiency based on two main influences which are the size of the span and the intensity of the external load-carrying capacity. The longer the span, the higher structural efficiency needed; the higher the load-carrying capacity, the lower the structural efficiency. These two influences are in fact different aspects of the same phenomenon, namely a requirement to maintain the ratio of selfweight to external load at a different load level (Macdonald, 2007)

In the case of a beam, the structural efficiency of element with a particular cross-sectional shape decreases as the span length increases. To maintain a constant level of efficiency over a range of spans, more efficient shapes of cross-sectional figure have to be utilized (Macdonald, 2007).

1.3 Types of steel section

Characteristic of the corrugated steel section and perforated steel section are described in the following sections.

1.3.1 Corrugated steel section

Corrugated steel webs have recently been proposed to replace the stiffened steel plates of plate girders as shown in Figure 1. 1 to improve the aesthetic design of the structure. Corrugated steel plates have been used as building and bridge components due to several advantages such as high shear resistance and out-of-plane stiffness.

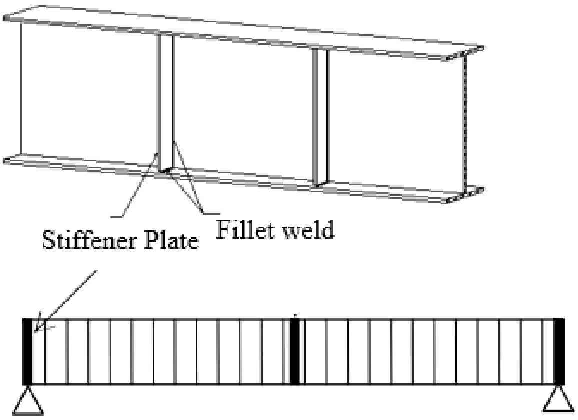

Figure 1.1 I-beam with stiffener plate (Sayed-Ahmed, 2007)

The usage of corrugated plates as the web I-girders can overcome the disadvantages of conventional stiffened flat webs such as web instability due to bending stress and also provide high fatigue resistance by minimization of the welding process (Moon et al., 2013). The corrugation profile can ensure higher resistibility against shear buckling, leading to the elimination of stiffeners (He et al., 2012). By eliminating the stiffener, hence, the cost of beam fabrication and the weight of structures could be reduced. Figure 1.2 shows the hexagonal sectional shape of the corrugated web profile used by Oh et al. (2012).

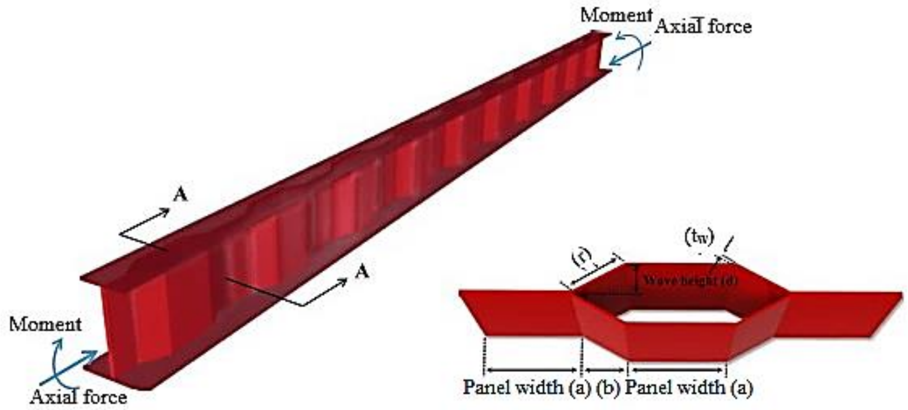

Figure 1.2 Profile of hexagonal sectional shape corrugated web (Oh et al., (2012))

The most commonly used corrugation profile for the corrugated web plate is the trapezoidal profile. The trapezoidal corrugated plates as shown in Figure 1.3 are composed of a series of plane and inclined sub-panels.

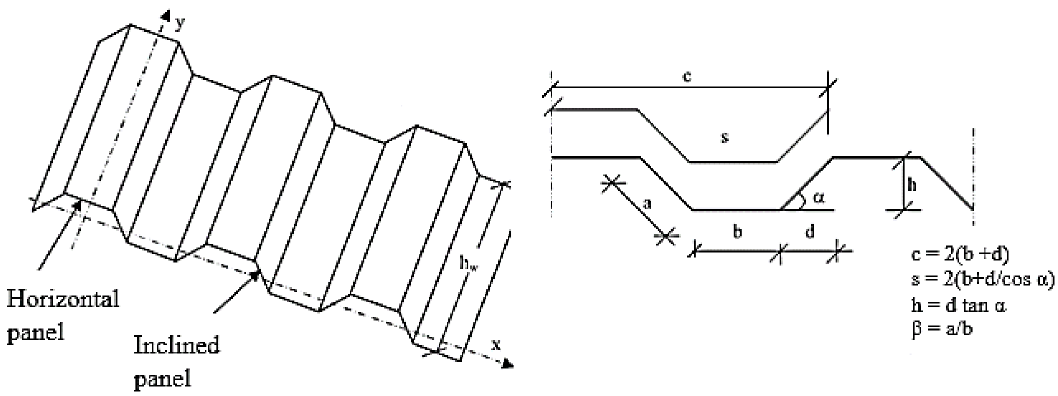

Figure 1.3 Trapezoidal profile of the corrugated web plates (Sayed-Ahmed, 2007)

The trapezoidal corrugated steel web provides enhanced buckling strength and weight saving by eliminating the stiffener (Eldib, 2009). Another innovation made by some researchers is by changing the corrugation web profile from trapezoidal to a curved corrugated web. Figure 1.4 shows the curved corrugated steel web designed by Eldib (2009), used for the design purposes of bridges structure.